The combination of residue quality, residue placement and soil mineral N content drives C and N dynamics by modifying N availability to microbial decomposers

Bruno Chaves, Marciel Redin, Sandro José Giacomini, Raquel Schmatz, Joël Léonard, Fabien Ferchaud, Sylvie Recous

The combination of residue quality, residue placement and soil mineral N content drives C and N dynamics by modifying N availability to microbial decomposers

Bruno Chaves [a,b], Marciel Redin [c], Sandro José Giacomini [a*], Raquel Schmatz[a], Joël Léonard [d], Fabien Ferchaud [d], Sylvie Recous [b*]

[a]*Department of Soils, Federal University of Santa Maria, 97105-900 Santa Maria, RS, Brazil*

[b]*Université de Reims Champagne Ardenne, INRAE, FARE, UMR A 614, Reims, 51097, France*

[c]*State University of Rio Grande do Sul, Unit Três Passos, 98600-000 Três Passos, RS, Brazil*

[d]*BioEcoAgro Joint Research Unit, INRAE, Université de Liège, Université de Lille, Université de Picardie Jules Verne, 02000 Barenton-Bugny, France*

corresponding author:

sylvie.recous@inrae.fr , UMR FARE, INRAE, 2 Esplanade Roland Garros, 51100, Reims, France

sjgiacomini@ufsm.br, Federal University of Santa Maria, 97105-900 Santa Maria, RS, Brazil

Highlights

- Crop residue quality and placement in soil interact during decomposition
- Soil surface placement and a high C:N ratio in residue reduce N availability to decomposers
- Low N availability decreases residue C mineralization and microbial N immobilization
- Residue degradation rate and biomass C:N ratio are controlled by the total N availability
- The N-limitation concept should improve predictions of net N mineralization.

Abstract:

Crop residues are the main source of carbon inputs to soils in cropping systems, and their subsequent decomposition is crucial for nutrient recycling. The interactive effects of residue chemical quality,

residue placement and soil mineral nitrogen (N) availability on carbon (C) and N mineralization dynamics were experimentally examined and interpreted using a modelling approach with the deterministic-functional, dynamic decomposition module of the Simulateur mulTIdisciplinaire pour les Cultures Standard (STICS) model. We performed a 120-day incubation at 25°C to evaluate how the mineralization of C and N from residues would respond to residue type (residues of 10 crop species with C:N ratios varying from 13 to 105), placement (surface or incorporated) and initial soil mineral N content (9 or 77 mg N kg^{-1} dry soil). A reduced C mineralization rate was associated with N limitation, as observed for high-C:N ratio residues, and shaped by residue placement and initial soil mineral N content. This was not observed for low-C:N ratio residues. Overall, increased net N mineralization corresponded with reduced N availability. Using the optimization procedure in the STICS decomposition module to explain the C and N dynamics of surface-decomposing residues, we estimated that 24% of the total soil mineral N would be accessible to decomposers. The STICS decomposition module reproduced the C and N dynamics for each treatment well after five parameters were optimized. The optimized values of the biomass C:N (*CNbio)*, residue decomposition rate (*k),* humification coefficient of microbial C *(h),* and microbial decomposition rate *(λ)* were significantly correlated with total N availability across all 40 treatments. Under low total N availability, *CNbio* increased, while *k*, *h* and *λ* decreased compared to their values under high N availability, suggesting functional changes in the microbial community of decomposers. Our results show that an N availability approach could be used to estimate residue C dynamics and net N mineralization in the field in response to crop residue quality and placement and demonstrate the potential to improve decomposition models by considering the effects of N availability on C dynamics.

Key words: chemical quality; crop residue; decomposition; N limitation; residue placement; STICS decomposition model

1. Introduction

The objectives of reducing reliance on mineral fertilizers as well as reactive nitrogen (N) losses in agrosystems and diversifying cropping systems (diversification of crops in rotation, double cropping, mixed cropping, reduction or suppression of soil tillage) have increased the need for an accurate method of predicting the decomposition dynamics of crop residues and their effect on carbon (C) fluxes and mineral N availability. C and N cycles are closely coupled during the microbial degradation of plant residues and litter in soils (Trinsoutrot et al., 2000; Li et al., 2013; Redin et al., 2014b). The intensity of C and N fluxes and the resulting net availability of mineral N in soils are controlled by the chemical characteristics of these substrates (Trinsoutrot et al., 2000; Liang et al., 2017) and the conditions of their decomposition, particularly the location of the residues in the soil and the environmental conditions (Coppens et al., 2006; Aita et al., 2012; Mulvaney et al., 2017).

Regarding residue placement, many studies have found that crop residues left on the soil surface decompose more slowly than incorporated residues (Curtin et al., 1998; Coppens et al., 2006; Mulvaney et al., 2017; Oliveira et al., 2020); this effect was attributed mainly to changes in conditions such as soil-residue contact and soil water content, which control decomposition (Coppens et al., 2007). The effect of the placement of crop residues on their decomposition rate has also been shown to depend on the nature of these residues; the decomposition of labile, N-rich residues (from immature plants) is little influenced by their initial placement (Bremer et al., 1991; Bending and Turner, 1999; Abiven and Recous, 2007). This finding suggests that N availability to decomposers, as influenced by soil-residue contact, is involved in the interaction between crop residue quality and placement (Giacomini et al., 2007; Li et al., 2013): N-rich residues contain and release N in sufficient amounts to sustain decomposition even if little N is available in the soil; in contrast, decomposition of N-poor residues is dependent on soil N, which, if not available (for example, when surface placement limits contact with the soil), becomes a limiting factor for decomposition. Studies examining the role of mineral N availability in C and N dynamics during decomposition showed that low N availability to decomposers not only slowed the rate of decomposition of N-poor (or high C:N) residues but also modified the amount of N assimilated per unit of decomposed C, suggesting the adaptation of

85 microbial communities of decomposers to N richness in their environment (Zechmeister-Boltenstern et
86 al., 2015). This could be due to a shift in the dominant microbial decomposer community (Nicolardot
87 et al., 2007) and/or the stoichiometric flexibility of the microorganisms (Agumas et al., 2021; Bai et
88 al., 2021). The effects of N availability on organic matter turnover have been more completely
89 described for soil humus than for plant residue decomposition, particularly in forest ecosystems
90 subjected to nitrogen enrichment (Chen et al., 2020; Geng et al., 2021). Few models have formalized
91 the relationships between crop residue decomposition and N availability during decomposition
92 (Molina et al., 1983; Li et al., 1992; Henriksen and Brelan, 1999a; Brisson et al., 2003). It can
93 therefore be seen that the overall availability of N to microbial decomposers, which impacts C
94 dynamics and the net mineralization of N, culminates in a given situation from three factors: the soil
95 and its mineral N content, the crop residue and its N content (organic and sometimes mineral), and the
96 colocation of the two sources of N (soil and residue) determined by residue placement, which affects
97 the greater or lesser accessibility of soil N to decomposers.

98 In this context, the objective of this work was to investigate the effect of the interaction
99 between the chemical quality of crop residues and their placement on residue decomposition, with a
100 focus on the role of N availability. To address this topic, we used an incubation approach to control all
101 experimental conditions, and we explored the responses obtained from 10 crop residues of different N
102 richness and biochemical composition that were left on the soil surface or incorporated into the soil;
103 the experimental soils had two initial levels of mineral N (abundant or limited). Manipulating the
104 initial mineral N content allowed us to disentangle the chemical quality and N richness of the residues
105 and to explore a wide range of N availability levels during decomposition. We hypothesized that the
106 placement of crop residues would first influence access to soil mineral N for decomposers and interact
107 with residue quality. We also tested the hypothesis that the soil mineral N, residue N and residue
108 placement as drivers of decomposition could be translated into a single variable, i.e., the overall N
109 availability to decomposers, across the wide range of residue types investigated. We used the
110 decomposition module of the Simulateur mulTIdisciplinaire pour les Cultures Standard (STICS)
111 model (Nicolardot et al., 2001) to interpret our experimental data, i.e., to estimate the functional
112 adaptations of the soil microbial biomass.

2. Materials and methods

2.1 Collection of plant material

Ten representative plant species grown as main crops or cover crops from agricultural systems in Brazil were studied (Table 1). The plants selected included four *Poaceae* (Gramineae), four *Fabaceae* (legumes), one *Brassicaceae*, and one *Asteraceae* species. The plants were cultivated in Typic Hapludalf soil under a no-till system in the experimental area (29°41′ S, 53°48′ W; approximately 90 m elevation) of the Soil Department of the Federal University of Santa Maria in the state of Rio Grande do Sul, Brazil. The region has a subtropical climate, with a mean annual precipitation of 1686 mm and a mean air temperature of 19.3°C. For the previous 12 years, the experimental site had been cultivated using a no-till system. All the crops were managed appropriately according to the technical recommendations for the area. The shoots of the plants were collected at flowering and harvest for the cover crop species and main crop species, respectively, and 3 replicates were obtained per species. The leaves that senesced before harvest were collected gradually until harvest, stored in paper bags and kept at room temperature. Subsequently, the plant shoots were separated into leaves and stems to determine their biomass proportion for each plant species (Table 1). The residues were first dried at 40°C, and the leaves and stems were then cut into pieces 1 cm in length. Subsequently, the residues were cut lengthwise into pieces with a thickness of approximately 0.5 and 0.3 cm for leaves and stems, respectively. A mixture of leaves and stems with a leaf: stem ratio similar to the ratio of dry biomass between leaves and stems determined under field conditions was also prepared (Table 1). One subsample of residue per species was dried at 40°C and ground to a size of 1 mm; a second subsample of each type of residue was dried at 65°C and finely ground (<1 mm) for chemical analyses.

2.2 Chemical characterization of plant residues

141 The total organic C and total N contents of the mixtures of leaves + stems were determined
142 from three finely ground subsamples dried at 65°C using an elemental autoanalyser (FlashEA 1112,
143 Thermo Finnigan, Milan, Italy). A proximate analysis using the Van Soest method was performed
144 using the subsamples of ground residues predried at 40°C. The soluble (SOL), cellulose (CEL),
145 hemicellulose (HEM), and lignin (LIG) fractions of the residues were determined by proximate
146 analysis (Van Soest, 1963) according to Redin et al. (2014a). The residues were placed in a 60-ml snap
147 cap vial with distilled water (20°C) and mechanically stirred for 30 min. After mixing, the material
148 was filtered (Whatman n° 5), and the contents of water-soluble organic C (Csw) and water-soluble
149 total N (Nsw) in the filtrate were determined. All analyses were performed with 3 replicates, and the
150 results are shown in Table 1.
151
152 *2.3 Soil, treatments, and experimental conditions*
153
154 The soil used was a Typic Hapludalf (USDA classification) collected from the 0–10-cm layer
155 in the no-till system. The soil contained 120 g kg^{-1} clay, 280 g kg^{-1} silt, 600 g kg^{-1} sand, 8.7 g kg^{-1}
156 organic C, and 0.9 g kg^{-1} total N and had a pH (H_2O) of 5.4. After visible organic residues had been
157 removed, the soil was sieved to 4 mm. Two initial mineral soil N levels were established for the
158 incubations: 1) 9 mg N kg^{-1} dry soil (low N availability; 9 N) and 2) 77 mg N kg^{-1} dry soil (high N
159 availability; 77 N). These levels were obtained by adding KNO_3-N prior to incubation to prevent N
160 limitation during decomposition (Recous et al., 1995). In the two treatments, the amount of water
161 added was calculated to achieve a soil moisture content of 80% of field capacity, i.e., 13.8 g H_2O 100
162 g^{-1} dry soil. The soils were preincubated in plastic bags at 25°C for 5 days.
163 The experiment consisted of incubation conducted for 120 days in the dark at 25 ± 1°C to
164 measure the C and N mineralization of the residue-amended soils. The experimental design consisted
165 of two sets of incubation jars prepared and monitored in parallel. One set of jars was used to evaluate
166 C-CO_2 emissions, and the second was used to measure the evolution of inorganic N in soils. The
167 treatments were arranged in a completely randomized design, and each treatment was replicated three
168 times. The residues, added at a rate of 0.56 g dry matter (DM) pot^{-1} (equivalent to 4.76 g DM per kg

dry soil), were either applied to the soil surface (S) or incorporated into the soil (I). This was equivalent to the addition of 1952 (oilseed rape) to 2155 (maize) mg C kg^{-1} of dry soil and 20 (maize) to 170 (vetch) mg N kg^{-1} of dry soil. To set up the pots for the experiment, a subsample of 134 g of moist soil was taken from each replicate. A subsample of 67 g of moist soil (S treatments) or soil mixed with half of the residues (I treatments) was then placed in a 110-ml cylindrical acrylic pot (5.0 cm in diameter and 5.0 cm in height) and compressed to a height of 2.5 cm. Then, a second subsample of 67 g of moist soil (S treatments) or soil mixed with half of the residues (I treatments) was placed in the same acrylic pot and packed to a total height of 5 cm. Thus, the soil in each pot reached a final bulk density of 1.2 g cm^{-3}. In the S treatments, the residues were homogeneously applied to the top of the soil in the pot. Treatments with soil and no residues were set up as controls. Each acrylic pot was placed in a 1000-ml glass jar prior to incubation.

2.4 Analytical procedures

C mineralization was assessed by quantifying continuous CO_2 release using NaOH trapping for samples taken at 2, 4, 7, 10, 14, 21, 28, 35, 50, 70, 90, and 120 days after the start of the incubation. The CO_2 produced in the soil was trapped in 10 ml of 1 M NaOH in a beaker placed inside each glass jar. The carbonate trapped in the NaOH was precipitated with a $BaCl_2$ solution in excess of 2 M, and the remaining NaOH was back-titrated with 1 M HCl. At all sampling times, the jars were aerated for 10 min to refresh the internal atmosphere, and the soil water content was checked by weighing and adjusted as necessary with a micropipette.

The soil mineral N content ($NH_4^+ + NO_2^- + NO_3^-$) was measured destructively on day 0 and at 7, 14, 21, 35, 63, 90 and 120 days of incubation. At each sampling time, the visible residual particles were removed. Mineral N was extracted from fresh soil samples with 1 M KCl (30 min shaking, soil-to-solution ratio 1:4). The soil KCl suspension was settled for 30 min until the supernatant liquid was clear, and the mineral N in an aliquot of the soil extracts was then measured by steam distillation (Keeney and Nelson, 1982). The jars were opened periodically, aerated and adjusted for humidity when necessary.

197

198 *2.5 Data and statistical analyses*

199

200 The apparent mineralization of C from the crop residues was calculated by subtracting the
201 amount of CO_2-C released with the control treatment from the amount of CO_2-C released with the
202 amended treatments. The apparent mineralization assumes that crop residue addition has no effect on
203 soil C mineralization (no priming effect) or that this effect is similar regardless of the type of crop
204 residue mixture added. Net N mineralization was calculated by subtracting the mineral N measured in
205 the control from the amount of mineral N that accumulated with each amended treatment (the same
206 control used to calculate the apparent C mineralization). The data on N mineralization and cumulative
207 C mineralization measured over 120 days were analysed by analysis of variance (ANOVA), and the
208 mean values were compared by the Tukey test ($p < 0.05$).

209 To obtain a quantitative measure of the relative importance of the initial chemical
210 characteristics of the residues for determining residue mineralization, we first calculated C
211 mineralization using an exponential equation according to Jung et al. (2011):

212 $$Cmin = C_0 (1 - e^{-b\,t}) \quad (1)$$

213 where $Cmin$ is the amount of mineralized carbon, C_0 is the potentially mineralizable C pool, b is the
214 total mineralization constant (crop residue and microbial biomass), and t is the incubation period.
215 Stepwise multiple regression analysis was then used to determine which combinations of chemical
216 variables best explained the variations in C_0 and b. Only those variables that were found to be
217 significant at $p < 0.05$ were retained in the regressions. Regressions were performed with all available
218 chemical variables of the residues.

219

220 *2.6 Modelling*

221 The decomposition module developed by Nicolardot et al. (2001) was used to analyse the
222 observed dynamics of C and N mineralization as affected by residue type, residue placement and
223 initial soil mineral N content. This decomposition module is part of the crop-soil model STICS
224 (Brisson et al., 2003), which is a dynamic, simple and robust model. The module was previously

parametrized under non-nitrogen-limited conditions from a dataset with a large range of crop residues that were finely ground and homogeneously incorporated into the soil (Nicolardot et al., 2001; Justes et al., 2009).

The module has three organic compartments: crop residue (*R*), decomposer microbial biomass (*B*) and humified organic matter (*H*). The crop residues and microbial biomass are assumed to decompose according to first-order kinetics with rate constants of k and λ (day^{-1}), respectively. The decomposed C is either mineralized as CO_2 or assimilated by the microbial biomass with yield efficiency Y ($g\ g^{-1}$). Microbial decay is assumed to result in C humification and secondary C mineralization at proportions of h and $1 - h$, respectively ($g\ g^{-1}$). The N dynamics are governed by the C transformation rates and the C:N ratios of the pools. The C and N fluxes are thus governed by seven parameters: two rate parameters (k and λ), two partitioning coefficients (Y and h) and three C:N ratios (those of the crop residue, the microbial biomass and the newly formed humified organic matter).

In the standard parameterization proposed by Nicolardot et al. (2001) and improved by Justes et al. (2009), the residue decomposition rate (k), the biomass C:N ratio (*CNbio*) and the humification coefficient of microbial C (h) are obtained using hyperbolic functions according to the residue C:N ratio (which is directly measured), while the rate of decomposition of microbial biomass (λ), the assimilation of residue C by the microbial biomass (Y) and the newly formed humified organic matter C:N (*CNhum*) are fixed and are therefore not related to the C:N ratio of the residue. This standard parameterization was obtained by nonlinear fitting and by minimizing the differences between observed and simulated apparent C and N mineralization from an incubation dataset including 43 different residues (Justes et al., 2009).

Although this module was originally parameterized and evaluated under non-nitrogen-limited conditions, Giacomini et al. (2007) found that it was able to reproduce observed data obtained under N limitation caused either by insufficient soil mineral N or by poor contact between soil and residues if certain decomposition parameters were modified. These authors proposed that three parameters (k, λ and *CNbio*) should be reoptimized and found that when N availability decreased, k and λ decreased, while *CNbio* increased. These principles were then incorporated into the STICS crop-soil model (v8 and later) by that addition of a cascade of effects under N-limited conditions: a reduction in the

253 decomposition rates (k, λ), an increase in the C:N of the microbial biomass and, if the availability of
254 the mineral N is still insufficient, an increase in the C:N of the newly formed humified organic matter.
255
256 *2.7 Model testing, parameter optimization and relationship with total N availability*
257
258 The 40 sets of apparent C and net N mineralization data obtained from the 10 crop residues
259 decomposing under 4 different conditions of residue placement and initial soil N content (I-77N, I-9N,
260 S-77N and S-9N) were compared with the simulations generated by the decomposition module. The
261 simulation process was organized into two steps: simulation with default values (standard
262 parameterization) and simulation after parameter optimization.
263 Simulations were first performed with the default parameter set established for incorporated
264 residues (Justes et al., 2009) to verify the ability of the STICS decomposition module to simulate the
265 present dataset.
266 Regarding the optimization process, we chose to limit the number of optimized parameters.
267 Our strategy was to build on the standard parameterization, only optimizing a small number of
268 parameters chosen according to previous works (Giacomini et al., 2007) and to literature describing
269 the relationship between N availability and the decomposition process (e.g., Mooshamer et al., 2014;
270 Manzoni et al., 2021). Indeed, we aimed not only to improve the model prediction of C and N
271 mineralization but also to express relationships between microbial traits and total N available to
272 decomposers. To do so, we tested three different scenarios with an increasing number of optimized
273 parameters. In each scenario, different model parameters were optimized simultaneously but
274 independently for each incubation treatment:
275 Scenario 1: k, λ, *CNbio*, *CNhum*. In *scenario 1*, we selected the parameters that were already
276 considered in the STICS soil-crop model to take into account the effect of low N availability on the
277 decomposition of crop residues. Indeed, the work by Giacomini et al. (2007) suggested that k and λ are
278 reduced with low N availability, while *CNbio* may increase. This was then incorporated into the
279 STICS soil-crop model, with the additional hypothesis that *CNhum* is ultimately affected if N

availability remains low. This first scenario therefore corresponds to how STICS manages the effect of N availability on decomposition.

Scenario 2: *k*, *λ*, *CNbio*, *CNhum, h*. For *scenario 2*, we added to the four parameters selected in *scenario 1* the humification rate of microbial biomass (*h*). In the standard parameterization, *h* varies according to the C:N ratio of the residue, which implies that residue quality affects the humification efficiency. In this scenario, we hypothesized that this parameter was affected not only by the C:N ratio of the residue but also more globally by the N availability (resulting from the C:N ratio of residue and from residue placement and soil N status).

Scenario 3: *k*, *λ, CNbio,* CNhum, *h, Y*. *Scenario 3* added the assimilation yield of residue C by microbial biomass (*Y*) to the five parameters optimized in *scenario 2*. Indeed, previous experimental works have shown that microbial carbon use efficiency can be affected by N availability (Manzoni et al., 2012): it tends to decrease when N availability is limited. Changes in *Y* according to N availability are considered in other decomposition models (e.g., Manzoni et al., 2021). The variation in *Y* during residue decomposition is associated with the higher energy investment and adaptation of microbial communities, which decrease under conditions of reduced N availability.

The optimization algorithm (Newton's method) available in Excel was used to minimize the deviations between the simulated and observed values. The minimization criterion was the RR (relative residual):

$$RR = \frac{RRMSE\,(C) + RRMSE\,(N)}{2}$$

with

$$RRMSE\,(A) = \sqrt{\frac{1}{n}\sum_{i=1}^{n}\left(\frac{A_i - \hat{A}_i}{max\,(A_i) - min\,(A_i)}\right)^2}$$

where RRMSE (*A*) represents the relative root mean square error for variable *A* (carbon or nitrogen mineralization from plant residues).

The maximum and minimum limits for each parameter except for *CNbio* and *CNhum* were those proposed by Nicolardot et al. (2001) ($0.05 \leq h \leq 1$; $0 \leq Y \leq 0.65$). *CNbio* had its upper limits

increased to 30 ($6 \leq CNbio \leq 30$) to take into account the possibility of stoichiometric flexibility of the fungal community (Cleveland and Liptzin, 2007; Camenzind et al., 2021). We considered that *CNhum* could vary between 8 and 12 ($8 \leq CNhum \leq 12$), which is consistent with the observed range of C:N of soil organic matter measured in cropped soils (e.g., Clivot et al., 2017). These parameters were assumed to be constant throughout the duration of the incubations. In all scenarios, the values of nonoptimized parameters were fixed or calculated according to their hyperbolic relationships with the C:N ratio of the residue (Justes et al., 2009).

The relationships between the observed and simulated data for C and N mineralization were evaluated using the root mean square error (RMSE):

$$RMSE(A) = \sqrt{\frac{1}{n}\sum_{i=1}^{n}(A_i - \hat{A}_i)^2}$$

The subsequent selection of the optimization scenario to interpret the effect of reduction of N availability on the decomposition process was made combining three criteria: i) the available knowledge of model parameters that are assumed to be dependent on the total N availability; ii) the resulting quality of prediction (RMSE), globally and for individual treatments; iii) and the quality of the relationship between optimized parameters and total N availability, to interpret the response of microbial traits to N availability.

2.7.3. Use of simulation results to estimate total N availability for decomposers

The main hypothesis of this work is that the interactive effects of residue type, residue placement, and soil initial mineral N content on the C and N mineralization of residues result from the overall N availability to decomposers. The total N availability was assumed to be the sum of the initial soil mineral N content plus the initial residue total N content. For the residue incorporation treatments, the soil mineral N in the soil core and the residue total N were assumed to be totally available to decomposers. For the surface residue application treatments, we assumed that only a fraction of the

initial soil mineral N content would be available to decomposers due to limited soil-residue contact, while all the residue N was considered potentially available. Therefore, the following calculations were aimed at estimating the plausible size of the soil mineral N fraction available to decomposers of surface-applied residues.

To estimate the size of this soil mineral N pool, the parameters *k*, *λ, h* and *CNbio* obtained in the optimization step (*scenario 2*) were plotted against the pool of N available to decomposers (total N availability), which was calculated separately for the incorporated and surface-applied residues. The plausible proportion of soil mineral N available for the decomposition of surface residues was determined using the Excel solver tool as the proportion allowing the best fit of the optimized parameters and the total N availability calculated for all treatments (incorporation and surface application).

3. Results

3.1 Crop residue characteristics

The residue C concentration varied slightly, from 421 g kg^{-1} DM (oilseed rape) to 453 g kg^{-1} (vetch), while the N concentration varied greatly, from 4.3 g kg^{-1} DM (maize) to 35.2 g kg^{-1} (vetch); therefore, the C:N ratios of the residues ranged from 13 to 105 (Table 1), with the C:N ratios of the cover crop residues in the low C:N range compared to the main crop residues. The LIG contents of the crop residues ranged from 61 g kg^{-1} DM (wheat) to 143 g kg^{-1} (soybean). In this dataset, the residue soluble DM concentration and total N concentration were strongly linearly correlated (r^2= 0.831), resulting from the crop maturity stage at which crop residues were harvested. Plants destroyed at the green stage, such as cover crops (black oat, showy rattlebox, gray mucuna and vetch), have cell vacuoles with both high soluble content and high N concentration, with the reverse when plants are mature (six other residues), due to the remobilization of carbon and nutrient reserves during grain-filling periods. Increased plant maturity is generally related to the deposition of lignocellulosic tissues (cellulose, hemicellulose and lignin) and governs the ratio of cytosoluble to cell wall fractions in plants (Bertrand et al., 2019), as observed here for the residues of the crops harvested at maturity.

359

360 *3.2 Global C and N mineralization patterns*

361 The cumulative C-CO_2 and net N mineralization from crop residues varied widely (Fig. 1).
362 The soil N availability, residue type and residue placement significantly affected the cumulative C
363 mineralization (P<0.05). The cumulative C mineralization (expressed as % added C) after 120 days
364 ranged from 39% (maize, S-9N) to 67% (black oat, S-77N) of the added C from surface residues and
365 from 43% (soybean, I-77N) to 66% (black oat and vetch, I-9N) of the added C from incorporated
366 residues (Fig. 1a,b). The mineral N dynamics indicated net immobilization or net mineralization in the
367 different treatments, and the values ranged from -26 mg N kg^{-1} soil (maize, S-9N) to +84 mg N kg^{-1}
368 soil (vetch, S-77N) with surface residues and from -30 mg N kg^{-1} soil (wheat, I-77N) to +100 mg N
369 kg^{-1} soil (vetch, I-9N) with incorporated residues (Fig. 1c,d).

370 The potentially mineralizable C pool (C_0) was calculated with a simple exponential decay
371 function and ranged from 40.7% added C (soybean; I-77N) to 66.6% added C (black oat; S-77N);
372 these values were close to the measured cumulative C mineralized over 120 days (Supplementary
373 Table S1). The mineralization constant (b) of C_0 differed among residues (Supplementary Table S1)
374 and ranged from 0.017 for maize (S-77N) to 0.126 for vetch (I-77N). A correlation analysis showed
375 that b was positively correlated with the residue N content (surface residues, r = 0.96; incorporated
376 residues, r = 0.97) and negatively correlated with CEL and HEM (surface residues, r = -0.84;
377 incorporated residues, r = -0.95). The potential mineralization pool (C_0) was correlated with the CEL,
378 HEM, and LIG contents, negatively correlated with surface residues (r = -0.35) and positively
379 correlated with incorporated residues (r = 0.55).

380 The C and N mineralization for the three crop residues (wheat, vetch, and oilseed rape) are
381 shown in Fig. 2 to illustrate the three main responses observed in the dataset (the values for the other
382 residues are presented in the supplementary material, Figs. S1 and S2). For wheat, the rate of C
383 mineralization was modified by the placement and availability of soil mineral N, with
384 I77>I9>S77>S9. This was not the case for vetch, for which the treatment had no effect on the initial C
385 mineralization; as the experiment continued, the C mineralization in the treatments slightly diverged,
386 with I9> I77 and S9 and S77 having intermediate values. For oilseed rape residue, there was no

387 difference in the kinetics of C mineralization regardless of the soil N availability or the initial residue
388 placement. The response typologies were very different for the net N mineralization in the soil. For
389 wheat, as expected from a residue with C:N=89, strong net N immobilization was observed throughout
390 the decomposition period (peaking at approximately -35 mg N kg^{-1} soil); N immobilization was more
391 pronounced and faster when the residues were incorporated and had a high initial mineral N content
392 (I77>I9>S77>S9). For the oilseed rape residue (C:N=22), N immobilization was more limited
393 (peaking at approximately -10 mg N kg^{-1} soil) and more transient in treatments I77 and I9, while only
394 positive net mineralization was observed in the S77 and S9 treatments, which had less mineral N in the
395 soil (S9>S77). For the vetch residues with a C:N ratio of 13, only net N mineralization was observed,
396 and there were no significant differences between treatments. On average, for all treatments, greater
397 net N immobilization was observed in the treatments with high initial soil mineral N (S-77N and I-
398 77N) than in the treatments with low initial soil mineral N (S-9N and I-9N).
399 To express the relationship between N and C dynamics and to compare treatments at similar
400 stages of decomposition, net N immobilization was expressed as a function of the cumulative C
401 mineralization for each treatment (Fig. 2g, h, i). The greatest net N immobilization was observed from
402 the incorporated residues of the *Poaceae* species, sunflower and soybean (mainly in the I-77N
403 treatment), when approximately 35% of the added residue C was mineralized (Fig. 2g and
404 Supplementary Figs. S1, S2). The residues decomposing at the soil surface immobilized less N than
405 the same residues incorporated into the soil at the same stage of decomposition (35% of the
406 cumulative residue C mineralized). The net N mineralization of residues with low initial C:N ratios
407 (vetch, gray mucuna) was not affected by the different treatments.
408
409 *3.3 Simulations with standard parameters and optimization scenarios*
410
411 Overall, C and N mineralization was not well simulated using the standard parameters of the
412 decomposition module developed under optimal conditions (finely ground residues and no N
413 limitation). As expected, the best simulation results were obtained for the residue incorporation
414 treatment with a high soil mineral N content (I-77N) (Figs. 3 and 4; Supplementary Figs. S1 and S2).

In this treatment, the lowest values of RMSE (C) and RMSE (N) were found for residues with low C:N ratios (vetch, I-77N and oilseed rape, I-77N). The same was observed for the surface-applied residues, and the lowest RMSE (C) and RMSE (N) were observed for the showy rattlebox residue in the treatment with high soil mineral N (S-77N) (Supplementary Fig. S1). In general, for the low soil N treatments (I-9N and S-9N), the model tended to overestimate C mineralization and underestimate net N mineralization, resulting in average RMSE values of 13.5% added C and 18.8 mg N kg^{-1} soil.

The parameter optimization performed in the three scenarios resulted in significant improvements in the simulations of C and N mineralization dynamics (Table 2). The RMSE (C) and RMSE (N) values decreased to averages of 2.48% added C and 2.04 mg N kg^{-1} for the three scenarios. The similar RMSE values obtained after optimization suggest that distinct decomposition model parameters lead to improved C and N mineralization predictions. However, *scenario 2* showed the most significant correlations between parameters and total N availability and therefore was selected to interpret the results (Fig. 5). Under *scenario 3,* no relationship was observed between *Y* and total N availability (Supplementary Fig. S3). In this scenario, the relationship between k, λ, and *CNbio* and the total N availability was slightly weakened compared to that with *scenario 2* (Supplementary Fig. S3), while *CNbio* values varied within the same range and were not markedly different between *scenario 2* and *scenario 3* (Supplementary Fig. S4).

3.4 Estimation of total N availability

For the residue incorporation treatments, the total N availability varied from 113.6 kg N (vetch, I-77) to 15.8 kg N (maize, I-9) per ton of residue C added (Supplementary Table S2). For the surface residue application treatments, using the parameter values generated through the optimization of *scenario 2*, the best fit between k, λ, h, and *CNbio* and the total N availability was obtained when 24% of the mineral N present in the soil was considered available to decomposers. This relationship resulted in significant correlations for k, λ, h and *CNbio* with total N available (Fig. 5). The calculated N availability ranged from 10.5 (maize, S-9N) to 86.3 (vetch, S-77N) kg N per ton of residue C added (Supplementary Table S2).

443

444 *3.5 Model optimization and effect of N availability*

445

446 The value of the parameter *k* optimized in *scenario 2* varied widely across the 10 residues × 4
447 treatments, from 0.02 to 0.23 day^{-1}, and increased with increasing total N availability (Fig. 5a)
448 regardless of the cause of the variation in total N availability (residue type or placement or initial soil
449 mineral N). The highest *k* values were observed for vetch residues; these varied little among the
450 different treatments (from 0.21 to 0.23 day^{-1} for I-77N and S-9N) because the main source of available
451 N for vetch was the residue N itself (Supplementary Table S2). For the mature residues with
452 intermediate to low N contents, *k* increased more drastically with increasing N availability, reflecting
453 the role of initial soil N and placement in the rate of C mineralization (Fig. 5). For example, for the
454 residues of barley and sunflower, *k* varied from 0.02–0.03 day^{-1} (S-9N) to 0.10–0.13 day^{-1} (I-77N)
455 (Supplementary Table S2).

456 The optimized parameter λ, which represents the decomposition rate of microbial biomass,
457 also increased with increasing total N availability (Fig 5). Higher values of λ were observed with
458 higher N residues (e.g., λ=0.038 and 0.030 day^{-1} for showy rattlebox and oilseed rape, respectively,
459 under I-77N) (Supplementary Table S2). Conversely, the lowest values of λ were observed for the
460 most mature residues with the lower N content, e.g., 0.003 and 0.002 day^{-1} for the maize and wheat S-
461 9N treatments, respectively (Fig. 5). However, the quality of fit obtained for these relationships was
462 much poorer than that for *k* (r = 0.48 vs. 0.86).

463 The optimized *CNbio* parameter showed a negative correlation with N availability and
464 decreased when the total N availability increased, with I-77N<I-9N<S-77N<S-9N (Fig. 5). *CNbio*
465 decreased from a maximal value of C:N=30 (wheat, barley, maize, sunflower in the S-9 treatments) at
466 low N availability to a minimum value of C:N= 8–11 at high N availability (gray mucuna, vetch,
467 showy rattlebox, oilseed rape in the I-77N & I-9N treatments). The parameter *h* decreased with
468 decreasing N availability, varying from 0.76 (showy rattlebox, I-77N) to 0.05 (residues with high C:N
469 ratios) (Supplementary Table S2). For immature residues with high N content, the *h* values remained
470 highly independent of residue placement and soil mineral N status (Fig. 5). The parameter *CNhum* was

also optimized in *scenario 2*; its values did not vary consistently and could not be correlated with the change in total N availability (data not shown). However, it was often higher in the I treatments than in the S treatments.

4. Discussion

4.1 Drivers of crop residue decomposition

The chemical characteristics and placement of crop residues and the soil mineral N content were shown in this study to be important drivers of residue decomposition. Considerable work has been done on these topics in the past, particularly on the relationship between crop residue quality and potential biodegradability (Trinsoutrot et al., 2000; Abiven et al., 2005; Harguindeguy et al., 2008; Redin et al., 2014b; Cyle et al., 2016). However, much less work has been done to unravel the effects of crop residue placement and its interaction with crop residue quality (Coppens et al., 2006; Li et al., 2013; Datta et al., 2019). Under field conditions, residue placement characterizes different agricultural management practices (tilled vs. no-tilled agroecosystems) that can affect the decomposition process by changing soil-residue contact, soil N availability and soil water dynamics (Arcand et al., 2016; Iqbal et al., 2015). Our study does not allow us to evaluate the effect of soil water dynamics on residue C and N mineralization. However, it is important to mention that in experimental situations with the potential for large water evaporation, dry conditions could also be a factor slowing down the decomposition of surface-applied residues compared to that of incorporated residues (Iqbal et al., 2015; Dietrich et al., 2019). It was previously shown that the chemical features of plant tissues (their proportions of various carbohydrate pools and their tissue architecture) and their N concentrations should be considered separately (Sall et al., 2007; Sukitprapanon et al., 2020). The former determines the intrinsic accessibility of plant cells to microorganisms and their enzymes and therefore drives the kinetics of degradation (Almagro et al., 2021). The latter, residue N, which is essential for microbial growth and metabolism, determines which of the two elements, C or N, is limiting; moreover, in soil,

498 residue N determines the balance between N immobilization and N mineralization (Yansheng et al.,
499 2020).

500 As observed in this study, the crop residue characteristics are mostly related to the maturation
501 stage of the plants, as crops used as cover crops (i.e., hairy vetch, gray mucuna, showy rattlebox and
502 oilseed rape in this study) were harvested in the vegetative stage, when they had low LIG contents and
503 high soluble DM and N concentrations. Therefore, the soluble DM pool and the total N concentration
504 were strongly and linearly correlated across the 10 plant residues, and the effects of these two residue
505 characteristics on C and N dynamics cannot be easily disentangled. The best treatments for examining
506 how the residue composition affects the dynamics of C mineralization were therefore those that
507 provided optimal conditions for decomposition, i.e., those in which the residues were incorporated into
508 soils with high initial mineral N levels (the I-77N treatments). The high mineral N availability
509 (corresponding on average to 37.0 ± 0.9 mg N g^{-1} added C) allowed the N-poor residues to overcome
510 N limitation, as the threshold for N limitation has been estimated to be approximately 30 mg N g^{-1}
511 added C according to Recous et al. (1995) and Mary et al. (1996). Under these non-N-limited
512 conditions, the kinetics of C mineralization exhibited biochemical differences between crop residues
513 (Trinsoutrot et al., 2000; Sall et al., 2007). Across the ten treatments, our results confirm a previously
514 noted pattern in which the degradation rate (*b*) is negatively correlated with the CEL and HEM
515 contents and positively correlated with the N and soluble DM contents (Redin et al., 2014b).
516 Conversely, the main driver of net N mineralization was the residue N content and the associated C:N
517 ratio. As expected (Abiven and Recous, 2007; Li et al., 2013; Yansheng et al., 2020), net N
518 mineralization was observed for residues with low C:N ratios, and N immobilization predominated for
519 residues with high C:N ratios.

520 One major finding of this study is the interaction of residue placement with residue quality and
521 how this interaction influences C and N dynamics. The placement of crop residues at the soil surface
522 has often been found to significantly decrease the rate of residue decomposition; for example, this was
523 observed by Coppens et al. (2006) with oilseed rape residue and by Datta et al. (2019) with rice and
524 wheat residues. However, it has also been shown (Schomberg et al., 1994) that this effect of residue
525 placement is dependent on the residue characteristics. Under laboratory conditions with controlled

temperature and moisture, this effect was attributed to poor soil-residue contact, which reduced the availability of soil mineral N for microbial biomass during decomposition of crop residues (Coppens et al. 2007). Our results confirm these findings, as the effect of residue placement was not observed for the residues with low C:N ratios in this study (vetch and oilseed rape residues). Conversely, surface placement drastically decreased the rates of mineralization of mature residues such as maize, wheat, sunflower, and barley to the extent that, at the end of the incubation, the dynamics of decomposition for surface maize residues with low mineral N (S-9N) was not advanced enough (maximal cumulative $C\text{-}CO_2$ = 39.4% C added) to initiate the phase of net N remineralization, which was observed fairly rapidly in all the other treatments.

In addition to modifying C mineralization kinetics, residue placement strongly influenced the intensity of N immobilization during decomposition and the net mineral N balance. Immobilization increased when residues were incorporated (incorporated > surface) for both soil mineral N levels, with 77N > 9N, e.g., for wheat and oilseed rape residues. The fact that incorporated residues promote N immobilization more than surface application was previously described by several authors (Giacomini et al., 2007; Aita et al., 2012; Mulvaney et al., 2017; Yansheng et al., 2020); the difference was more pronounced with high-C:N ratio residues, confirming our results. With intermediate-C:N ratio residues (e.g., oilseed rape and showy rattlebox), despite the lack of an effect of placement on C mineralization, net N immobilization was observed when the residues were incorporated, while only net N mineralization was observed when the residues were left on the soil surface. This pattern suggests differences in microbial N consumption during decomposition, even in treatments with no N limitation on C degradation (i.e., the vetch and gray mucuna treatments). This reduction in N consumption by decomposers for a given amount of decomposed C was previously highlighted by Recous et al. (1995) and Mary et al. (1996), who demonstrated with maize and wheat residues a threshold of N availability below which microbial N consumption per unit of mineralized C was lower but the straw C mineralization rate was unchanged. In their work, the microbial N immobilization rate varied from 30 mg N g^{-1} C mineralized under high N availability conditions to 11–15 mg N g^{-1} C mineralized under N-limited conditions (Mary et al., 1996). Therefore, our results, which were obtained with a large range of residue qualities, confirm the important role of N availability in the

554 dynamics of residue C mineralization and N mineralization; N availability is modulated by the
555 interaction between crop residue composition, crop residue placement and initial soil mineral N, which
556 are drivers that interact to determine the overall N availability to decomposers. We believe that the
557 conditions that control the degradation of crop residues by the availability of mineral N are very
558 common in field conditions, especially in cereal systems, where large amounts of straw may be left in
559 the field, either on the soil surface as mulch (no-till systems) or incorporated into the topsoil layer by
560 reduced-tillage techniques, while the soil layer concerned does not contain the amounts of mineral N
561 corresponding to the microbial needs created by straw incorporation. Limited soil-residue contact and
562 access to mineral N are also affected by the size of the residue particles, and larger particles (decimetre
563 size range, such in that observed the field) induce heterogeneity of distribution in the soil and
564 potentially slow decomposition (e.g., Iqbal et al., 2014). To unravel the response of microbial biomass
565 to N limitation in terms of metabolic traits, this assumption was further tested using a modelling
566 approach.
567
568 *4.2 Conceptual approach to determining the overall N availability to decomposers*
569 Few studies have proposed a conceptual approach for determining the accessibility of soil
570 mineral N from a crop residue layer left on the soil surface. Some models that take into account the
571 possible N control of decomposition introduced a parameter that defines the thickness of the
572 underlying soil that "feeds" the decaying mulch (Findeling et al., 2007; Balwinder-Singh et al., 2011).
573 Some work has also demonstrated the biological realities of these processes by observing either
574 nutrient translocation by fungal hyphae (George et al., 1992) or the N diffusion gradient in the soil,
575 e.g., in the detritusphere (Gaillard et al., 1999). The observed differences between the S77 and S9
576 treatments indicate that the amount of mineral N under the residue layer influenced their
577 decomposition, revealing the contribution of soil N to decomposition. Here, we adopted an empirical
578 approach using the STICS decomposition module (Nicolardot et al., 2001) that was based on
579 optimization of the microbial parameters *k, λ, h, CNbio* and *CNhum* to determine the plausible size of
580 the soil N pool that is accessible to decomposers under surface decomposition conditions. Across the
581 ten crop residues and the two initial levels of mineral N (9 and 77 mg N kg^{-1} dry soil), the best fit

582 between the observed and simulated C and N dynamics was obtained by considering that 24% of the
583 soil mineral N was accessible to decomposers during surface residue decomposition; this corresponded
584 to an approximately 1.25-cm soil depth in the soil pots used in the present work. Such an estimation
585 allowed us to calculate the total N availability for the 40 treatments tested.
586
587 *4.3 Effects of N availability on the modelled parameters of microbial biomass*
588 The independent optimization of the STICS module parameters for each residue × treatment
589 combination indicated a reduction in the residue decomposition rate *(k)*, an increase in the C:N ratio of
590 microbial biomass *(CNbio)*, a decrease in decomposer microbial biomass decay *(λ)* and a reduction in
591 humification *(h)* when N availability was reduced; optimizing the assimilation yield parameter (*Y*) did
592 not improve the simulations and did not significantly change the range of *CNbio* values. The most
593 notable result was that each of these four parameters exhibited a relationship with the total available N,
594 regardless of crop residue, residue placement or initial soil mineral N content; this confirms our initial
595 hypothesis of the relevance of the conceptual approach based on total N availability. This relationship
596 to N availability was particularly strong for *k* and *CNbio*.
597 Evidence of a reduction in the residue decomposition rate under conditions of low N
598 availability was observed by other authors (Henriksen and Breland, 1999b; Hadas et al., 2004; Wang
599 et al., 2004; Delgado-Baquerizo et al., 2015). The lower the C:N ratio of the residues was, the lower
600 the reduction in the decomposition rate. These results show the same substantial effect of reduced N
601 availability on high-C:N ratio residues, as observed by Schomberg et al. (1994), who found greater
602 changes in the decomposition rate between incorporated and surface-applied grain sorghum and wheat
603 residues than between incorporated and surface-applied alfalfa residues. The decomposer microbial
604 biomass decay *(λ)* was also reduced under conditions of low total N availability. In the Henriksen and
605 Breland (1999a) model, the decay rate constant of the microbial biomass changed for different organic
606 pools (plant decomposable, plant structural and humus pools) and decreased with the increase in the
607 N-deficient structural material.
608 We also noted an increase in humification (*h)* with increasing N availability, which is in
609 agreement with the initial soil mineral N-limitation formalism of the model (Justes et al., 2009) but

610 also takes into account the N limitation linked to residue placement. These results reinforce the
611 importance of microbial biomass as a precursor to stable soil organic matter (Alvarez and Alvarez,
612 2000; Liang et al., 2019; Wang et al., 2020). The higher humification rate observed for low-C:N ratio
613 residues is related to their large soluble DM fractions, which are rapidly assimilated by microbial
614 biomass but are also available for the stabilization and formation of soil mineral-associated organic
615 matter (MAOM) (Cyle et al., 2016). Residues with a high C:N ratio contain a higher percentage of
616 complex polymers (e.g., cellulose and hemicellulose), resulting in fewer compounds that can be
617 stabilized as MAOM (Almagro et al., 2021).

618 An increase in the C:N ratio of microbial biomass when N availability is reduced has been
619 included in other models (Blagodatsky and Richter, 1998; Henriksen and Brelan, 1999a; Manzoni et
620 al. 2021). This increase implicitly reflects a change in the microbial community structure of
621 decomposers that is probably related to the higher contribution of fungi to decomposition. The
622 maximal C:N value of the microbial biomass (here, $CNbio \leq 30$) is an optimized parameter of a simple
623 model and does not necessarily reflect a biological reality; however, variations in microbial biomass
624 C:N ratios appear on average rather constrained, at 8.6 ± 0.3 according to Cleveland and Liptzin
625 (2007), but ranged between 3 and 24 in their study. Evidence for some stoichiometric flexibility of
626 microbial communities was also shown by Li et al. (2012) and Fanin et al. (2013). Fungi exhibit lower
627 metabolic activity than bacteria as well as highly efficient N use (Zechmeister-Boltenstern et al.,
628 2015). Their filamentous hyphae can provide access to soil resources through the remobilization and
629 transfer of N, allowing surface residues to decompose under conditions of low N availability (Frey et
630 al., 2000). Camenzind et al. (2021) demonstrated the high flexibility of the C:N ratio of soil fungal
631 mycelia in conditions of varied N availability, varying their C:N ratio from 8–18 (high N supply) to 84
632 (low N supply). Another possible explanation for the change in C:N ratios is that the C-use efficiency
633 or assimilation yield (Y) decreases with decreased N availability, consequently decreasing the N
634 requirements of the microbial community by modifying their cellular composition according to the
635 external nutrient availability (Sinsabaugh et al., 2013; Manzoni et al., 2021;). In this study,
636 optimization *scenario 3*, which had varying Y values, did not result in a good overall correlation with
637 N availability and could not explain the lower N immobilization observed in the low N availability

638 treatments. Although the closest correlation to N availability was found using a fixed value of *Y* with
639 STICS (0.62), Sinsabaugh et al. (2013) recommended using a value of 0.30 for C-use efficiency in
640 large-scale models and a variable *Y* value for small-scale models. The literature shows evidence of
641 changes in *Y* with decreasing N availability (Agumas et al., 2021; Bai et al., 2021), which can also be
642 linked to changes in the microbial community (Bölscher et al., 2016); however, as a result of the
643 simplicity of the model and the optimization procedure, the model could compensate for the variation
644 in *Y* by increasing *CNbio*, which still indicates a modification in the soil microbial decomposer
645 community. Manzoni et al. (2021) showed that the response of microbial adaptation to N limitation
646 should be done by different mechanisms: flexible C-use efficiency, selective enzymes, the plastic
647 microbial biomass C:N ratio, and nutrient retention in the microbial biomass. The authors conclude
648 that all four mechanisms could be used during microbial adaptation to low N availability.
649
650 **5. Conclusion**
651 A combination of incubation experiments and modelling showed for the first time, across a
652 large range of crop residue types, how the combination of residue chemical quality, residue placement
653 and soil mineral N content drives C and N dynamics by modifying N access for microbial
654 decomposers, defined in this work as the total N availability. The placement of residues on the soil
655 surface imposes a limitation on soil N resources for microbial decomposer biomass. This limitation is
656 critical for high-C:N ratio residues but less important or negligible for low-C:N ratio residues. The use
657 of a modelling approach allowed the possibility of exploring the effects of these interactions on
658 microbial biomass functional traits and understanding the unique C and N mineralization patterns
659 observed. The reduction in total N availability led to a reduction in residue decomposition, microbial
660 biomass decay and humification rates and to an increase in the C:N ratio of microbial biomass. These
661 parameter changes were more notable for high-C:N ratio residues than for low-C:N ratio residues, for
662 which the high residue N content was the main source of N for microorganism metabolism,
663 independent of residue placement and soil mineral N status. The N availability approach appears to be
664 appropriate for predicting the dynamics of N mineralization after crop residue recycling under
665 management conditions where available N can often be a driver of organic matter decomposition, such

as under reduced- or no-tillage field conditions with, e.g., cereal straw. However, this approach needs to be further tested at the field level under different N-limitation conditions. Further work should be done first by implementing or improving N-limitation functions in C-N decomposition models and then combining experiments and modelling under field conditions.

Acknowledgements

This work was supported by the Brazilian government through the Coordenação de Aperfeiçoamento de Pessoal de Nível Superiror – Brasil (CAPES) – Finance Code 001. Funding for the bilateral Brazilian and French collaboration was provided under Program CAPES-PRINT – Programa Institucional De Internacionalização, Process Number 88887.373791/2019–00, and by INRAE (the French National Research Institute for Agriculture, Food and Environment) to SR, JL and FF and by URCA (Université de Reims Champagne Ardenne) during BC's leave at UMR FARE in Reims, France.

References

Abiven, S., Recous, S., 2007. Mineralisation of crop residues on the soil surface or incorporated in the soil under controlled conditions. Biology and Fertility of Soils 43, 849–852. doi:10.1007/s00374-007-0165-2

Abiven, S., Recous, S., Reyes, V., Oliver, R., 2005. Mineralisation of C and N from root, stem and leaf residues in soil and role of their biochemical quality. Biology and Fertility of Soils 42, 119–128. doi:10.1007/s00374-005-0006-0

Agumas, B., Blagodatsky, S., Balume, I., Musyoki, M.K., Marhan, S., Rasche, F., 2021. Microbial carbon use efficiency during plant residue decomposition: Integrating multi-enzyme stoichiometry and C balance approach. Applied Soil Ecology 159, 103820. doi:10.1016/j.apsoil.2020.103820

Aita, C., Recous, S., Cargnin, R.H.O., da Luz, L.P., Giacomini, S.J., 2012. Impact on C and N dynamics of simultaneous application of pig slurry and wheat straw, as affected by their initial locations in soil. Biology and Fertility of Soils 48, 633–642. doi:10.1007/s00374-011-0658-x

Almagro, M., Ruiz-navarro, A., Díaz-pereira, E., Albaladejo, J., Martínez-Mena, M., 2021. Plant residue chemical quality modulates the soil microbial response related to decomposition and soil organic carbon and nitrogen stabilization in a rainfed Mediterranean agroecosystem. Soil Biology and Biochemistry 156, 108198. doi:10.1016/j.soilbio.2021.108198

Alvarez, R., Alvarez, C.R., 2000. Soil Organic Matter Pools and Their Associations with Carbon Mineralization Kinetics. Soil Science Society of America Journal 64, 184–189.

701 Arcand, M.M., Helgason, B.L., Lemke, R.L., 2016. Microbial crop residue decomposition dynamics in
702 organic and conventionally managed soils. Applied Soil Ecology 107, 347–359.
703 doi:10.1016/j.apsoil.2016.07.001

704 Bai, X., Dippold, M.A., An, S., Wang, B., Zhang, H., Loeppmann, S., 2021. Extracellular enzyme
705 activity and stoichiometry: The effect of soil microbial element limitation during leaf litter
706 decomposition. Ecological Indicators 121, 107200. doi:10.1016/j.ecolind.2020.107200

707 Balwinder-Singh, Gaydon, D.S., Humphreys, E., Eberbach, P.L., 2011. The effects of mulch and
708 irrigation management on wheat in Punjab, India-Evaluation of the APSIM model. Field Crops
709 Research 124, 1–13. doi:10.1016/j.fcr.2011.04.016

710 Bending, G.D., Turner, M.K., 1999. Interaction of biochemical quality and particle size of crop
711 residues and its effect on the microbial biomass and nitrogen dynamics following incorporation
712 into soil. Biology and Fertility of Soils 29, 319–327. doi:10.1007/s003740050559

713 Bertrand, I., Viaud, V., Daufresne, T., Pellerin, S., Recous, S., 2019. Stoichiometry constraints
714 challenge the potential of agroecological practices for the soil C storage. A review. Agronomy
715 for Sustainable Developtment 39, 1–16.

716 Blagodatsky, S.A., Richter, O., 1998. Microbial growth in soil and nitrogen turnover: a theoretical
717 model considering the activity state of microorganisms. Soil Biology and Biochemistry 30,
718 1743–1755. doi:10.1016/S0038-0717(98)00028-5

719 Bölscher, T., Wadsö, L., Börjesson, G., Herrmann, A.M., 2016. Differences in substrate use
720 efficiency: impacts of microbial community composition, land use management, and substrate
721 complexity. Biology and Fertility of Soils 52, 547–559. doi:10.1007/s00374-016-1097-5

722 Bremer, E., van Houtum, W., van Kessel, C., 1991. Carbon dioxide evolution from wheat and lentil
723 residues as affected by grinding, added nitrogen, and the absence of soil. Biology and Fertility of
724 Soils 11, 221–227. doi:10.1007/BF00335771

725 Brisson, N., Gary, C., Justes, E., Roche, R., Mary, B., Ripoche, D., Zimmer, D., Sierra, J., Bertuzzi, P.,
726 Burger, P., Bussière, F., Cabidoche, Y.., Cellier, P., Debaeke, P., Gaudillère, J.., Hénault, C.,
727 Maraux, F., Seguin, B., Sinoquet, H., 2003. An overview of the crop model stics. European
728 Journal of Agronomy 18, 309–332. doi:10.1016/S1161-0301(02)00110-7

729 Camenzind, T., Grenz, K.P., Lehmann, J., Rillig, M.C., 2021. Soil fungal mycelia have unexpectedly
730 flexible stoichiometric C:N and C:P ratios. Ecology Letters 24, 208–218. doi:10.1111/ele.13632

731 Chen, J., Xiao, W., Zheng, C., Zhu, B., 2020. Nitrogen addition has contrasting effects on particulate
732 and mineral-associated soil organic carbon in a subtropical forest. Soil Biology and Biochemistry
733 142, 107708. doi:10.1016/j.soilbio.2020.107708

734 Cleveland, C.C., Liptzin, D., 2007. C:N:P stoichiometry in soil: is there a "'Redfield ratio"' for the
735 microbial biomass? Biogeochemistry 85, 235–252. doi:10.1007/s10533-007-9132-0

736 Clivot, H., Mary, B., Valé, M., Cohan, J., Champolivier, L., Piraux, F., Laurent, F., Justes, E., 2017.
737 Quantifying in situ and modeling net nitrogen mineralization from soil organic matter in arable
738 cropping systems. Soil Biology & Biochemistry 111, 44–59. doi:10.1016/j.soilbio.2017.03.010

739 Coppens, F., Garnier, P., De Gryze, S., Merckx, R., Recous, S., 2006. Soil moisture, carbon and
740 nitrogen dynamics following incorporation and surface application of labelled crop residues in
741 soil columns. European Journal of Soil Science 57, 894–905. doi:10.1111/j.1365-
742 2389.2006.00783.x

743 Coppens, F., Garnier, P., Findeling, A., Merckx, R., Recous, S., 2007. Decomposition of mulched
744 versus incorporated crop residues: Modelling with PASTIS clarifies interactions between residue

quality and location. Soil Biology and Biochemistry 39, 2339–2350. doi:10.1016/j.soilbio.2007.04.005

Curtin, D., Selles, F., Wang, H., Biederbeck, V.O., Campbell, C.A., 1998. Carbon Dioxide Emissions and Transformation of Soil Carbon and Nitrogen during Wheat Straw Decomposition. Soil Science Society of America Journal 62, 1035–1041. doi:10.2136/sssaj1998.03615995006200040026x

Cyle, K.T., Hill, N., Young, K., Jenkins, T., Hancock, D., Schroeder, P.A., Thompson, A., 2016. Substrate quality influences organic matter accumulation in the soil silt and clay fraction. Soil Biology and Biochemistry 103, 138–148. doi:10.1016/j.soilbio.2016.08.014

Datta, A., Jat, H.S., Yadav, A.K., Choudhary, M., Sharma, P.C., Rai, M., Singh, L.K., Majumder, S.P., Choudhary, V., Jat, M.L., 2019. Carbon mineralization in soil as influenced by crop residue type and placement in an Alfisols of Northwest India. Carbon Management 10, 37–50. doi:10.1080/17583004.2018.1544830

Delgado-Baquerizo, M., García-Palacios, P., Milla, R., Gallardo, A., Maestre, F.T., 2015. Soil characteristics determine soil carbon and nitrogen availability during leaf litter decomposition regardless of litter quality. Soil Biology and Biochemistry 81, 134–142. doi:10.1016/j.soilbio.2014.11.009

Dietrich, G., Recous, S., Pinheiro, P.L., Weiler, D.A., Schu, A.L., Rambo, M.R.L., Giacomini, S.J., 2019. Gradient of decomposition in sugarcane mulches of various thicknesses. Soil & Tillage Research 192, 66–75. doi:10.1016/j.still.2019.04.022

Fanin, N., Fromin, N., Buatois, B., Hättenschwiler, S., 2013. An experimental test of the hypothesis of non-homeostatic consumer stoichiometry in a plant litter – microbe system. Ecology Letters 16, 764–772. doi:10.1111/ele.12108

Findeling, A., Garnier, P., Coppens, F., Lafolie, F., Recous, S., 2007. Modelling water, carbon and nitrogen dynamics in soil covered with decomposing mulch. European Journal of Soil Science 58, 196–206. doi:10.1111/j.1365-2389.2006.00826.x

Frey, S.D., Elliott, E.T., Paustian, K., Peterson, G.A., 2000. Fungal translocation as a mechanism for soil nitrogen inputs to surface residue decomposition in a no-tillage agroecosystem. Soil Biology and Biochemistry 32, 689–698. doi:10.1016/S0038-0717(99)00205-9

Gaillard, V., Chenu, C., Recous, S., Richard, G., 1999. Carbon, nitrogen and microbial gradients induced by plant residues decomposing in soil. European Journal of Soil Science 50, 567–578. doi:10.1046/j.1365-2389.1999.00266.x

Geng, J., Fang, H., Cheng, S., Pei, J., 2021. Effects of N deposition on the quality and quantity of soil organic matter in a boreal forest: Contrasting roles of ammonium and nitrate. Catena 198, 104996. 104996. doi:10.1016/j.catena.2020.104996

George, E., Häussler, K.-U., Vetterlein, D., Gorgus, E., Marschner, H., 1992. Water and nutrient translocation by hyphae of Glomus mosseae. Canadian Journal of Botany 70, 2130–2137. doi:10.1139/b92-265

Giacomini, S.J., Recous, S., Mary, B., Aita, C., 2007. Simulating the effects of N availability, straw particle size and location in soil on C and N mineralization. Plant and Soil 301, 289–301. doi:10.1007/s11104-007-9448-5

Hadas, A., Kautsky, L., Goek, M., Erman Kara, E., 2004. Rates of decomposition of plant residues and available nitrogen in soil, related to residue composition through simulation of carbon and nitrogen turnover. Soil Biology and Biochemistry 36, 255–266. doi:10.1016/j.soilbio.2003.09.012

790 Harguindeguy, N.P., Blundo, C.M., Gurvich, D.E., Díaz, S., Cuevas, E., 2008. More than the sum of
791 its parts? Assessing litter heterogeneity effects on the decomposition of litter mixtures through
792 leaf chemistry. Plant and Soil 303, 151–159. doi:10.1007/s11104-007-9495-y

793 Henriksen, T., Brelan, 1999a. Evaluation of criteria for describing crop residue degradability in a
794 model of carbon and nitrogen turnover in soil. Soil Biology and Biochemistry 31, 1135–1149.
795 doi:10.1016/S0038-0717(99)00031-0
796
797 Henriksen, T.M., Breland, T.A., 1999b. Nitrogen availability effects on carbon mineralization, fungal
798 and bacterial growth, and enzyme activities during decomposition of wheat straw in soil. Soil
799 Biology and Biochemistry 31, 1121–1134. doi:10.1016/S0038-0717(99)00030-9

800 Iqbal, A., Aslam, S., Alavoine, G., Benoit, P., Garnier, P., Recous, S., 2015. Rain regime and soil type
801 affect the C and N dynamics in soil columns that are covered with mixed-species mulches. Plant
802 and Soil 393, 319–334. doi:10.1007/s11104-015-2501-x

803 Iqbal, A., Garnier, P., Lashermes, G., Recous, S., 2014. A new equation to simulate the contact
804 between soil and maize residues of different sizes during their decomposition. Biology and
805 Fertility of Soils 50, 645–655. doi:10.1007/s00374-013-0876-5

806 Jung, J.Y., Lal, R., Ussiri, D.A.N., 2011. Changes in CO2, 13C abundance, inorganic nitrogen, β-
807 glucosidase, and oxidative enzyme activities of soil during the decomposition of switchgrass root
808 carbon as affected by inorganic nitrogen additions. Biology and Fertility of Soils 47, 801–813.
809 doi:10.1007/s00374-011-0583-z

810 Justes, E., Mary, B., Nicolardot, B., 2009. Quantifying and modelling C and N mineralization kinetics
811 of catch crop residues in soil: parameterization of the residue decomposition module of STICS
812 model for mature and non mature residues. Plant and Soil 325, 171–185. doi:10.1007/s11104-
813 009-9966-4

814 Keeney, D.R., Nelson, D.W., 1982. Nitrogen in organic forms. In: Page, A.L. (Ed.), Methods of Soil
815 Analysis, Part 2. Agronomy Monograph, second ed. ASA and SSSA, Madison, WI, pp. 643-698.

816 Li, C., Frolking, S., Frolking, T.. A., 1992. A Model of Nitrous Oxide Evolution From Soil Driven by
817 Rainfall Events: 1 . Model Structure and Sensitivity. Journal of Geophysical Research 97, 9759–
818 9776.

819 Li, L.-J., Han, X.-Z., You, M.-Y., Yuan, Y.-R., Ding, X.-L., Qiao, Y.-F., 2013. Carbon and nitrogen
820 mineralization patterns of two contrasting crop residues in a Mollisol: Effects of residue type and
821 placement in soils. European Journal of Soil Biology 54, 1–6. doi:10.1016/j.ejsobi.2012.11.002

822 Li, Y., Wu, J., Liu, S., Shen, J., Huang, D., Su, Y., Wei, W., Syers, J.K., 2012. Is the C:N:P
823 stoichiometry in soil and soil microbial biomass related to the landscape and land use in southern
824 subtropical China? Global Biogeochemical Cycles 26, 1–14. doi:10.1029/2012GB004399

825 Liang, C., Amelung, W., Lehmann, J., Kästner, M., 2019. Quantitative assessment of microbial
826 necromass contribution to soil organic matter. Global Change Biology 25, 3578–3590.
827 doi:10.1111/gcb.14781

828 Liang, X., Yuan, J., Yang, E., Meng, J., 2017. Responses of soil organic carbon decomposition and
829 microbial community to the addition of plant residues with different C:N ratio. European Journal
830 of Soil Biology 82, 50–55. doi:10.1016/j.ejsobi.2017.08.005

831 Manzoni, S., Chakrawal, A., Spohn, M., Lindahl, B.D., 2021. Modeling Microbial Adaptations to
832 Nutrient Limitation During Litter Decomposition. Frontiers in Forests and Global Change 4, 1–
833 23. doi:10.3389/ffgc.2021.686945

834 Mary, B., Recous, S., Darwis, D., Robin, D., 1996. Interactions between decomposition of plant

residues and nitrogen cycling in soil. Plant and Soil 181, 71–82. doi:10.1007/BF00011294

Molina, J.A.E., Clapp, C.E., Shaffer, M.J., Chichester, F.W., Larson, W.E., 1983. NCSOIL, A Model of Nitrogen and Carbon Transformations in Soil: Description, Calibration, and Behavior. Soil Science Society of America Journal 47, 85–91.

Mooshammer, M., Wanek, W., Zechmeister-boltenstern, S., Richter, A., 2014. Stoichiometric imbalances between terrestrial decomposer communities and their resources: mechanisms and implications of microbial adaptations to their resources. Frontiers in Microbiology 5, 1–10. doi:10.3389/fmicb.2014.00022

Mulvaney, M.J., Balkcom, K.S., Wood, C.W., Jordan, D., 2017. Peanut Residue Carbon and Nitrogen Mineralization under Simulated Conventional and Conservation Tillage. Agronomy Journal 109, 696–705. doi:10.2134/agronj2016.04.0190

Nicolardot, B., Bouziri, L., Bastian, F., Ranjard, L., 2007. A microcosm experiment to evaluate the influence of location and quality of plant residues on residue decomposition and genetic structure of soil microbial communities. Soil Biology and Biochemistry 39, 1631–1644. doi:10.1016/j.soilbio.2007.01.012

Nicolardot, B., Recous, S., Mary, B., 2001. Simulation of C and N mineralisation during crop residue decomposition: A simple dynamic model based on the C:N ratio of the residues. Plant and Soil 228, 83–103. doi:10.1023/A:1004813801728

Oliveira, M., Rebac, D., Coutinho, J., Ferreira, L., Trindade, H., 2020. Nitrogen mineralization of legume residues: interactions between species, temperature and placement in soil. Spanish Journal of Agricultural Research 18, 1–11. doi:10.5424/sjar/2020181-15174

Recous, S., Robin, D., Darwis, D., Mary, B., 1995. Soil inorganic N availability: Effect on maize residue decomposition. Soil Biology and Biochemistry 27, 1529–1538. doi:10.1016/0038-0717(95)00096-W

Redin, M., Guénon, R., Recous, S., Schmatz, R., Freitas, L.L. De, Aita, C., Giacomini, S.J., 2014a. Carbon mineralization in soil of roots from twenty crop species, as affected by their chemical composition and botanical family. Plant Soil 378, 205–214. doi:10.1007/s11104-013-2021-5

Redin, M., Recous, S., Aita, C., Dietrich, G., Caitan, A., Hytalo, W., Schmatz, R., Jos, S., 2014b. How the chemical composition and heterogeneity of crop residue mixtures decomposing at the soil surface affects C and N mineralization. Soil Biology & Biochemistry 78, 65–75. doi:10.1016/j.soilbio.2014.07.014

Sall, S., Bertrand, I., Chotte, J.L., Recous, S., 2007. Separate effects of the biochemical quality and N content of crop residues on C and N dynamics in soil. Biology and Fertility of Soils 43, 797–804. doi:10.1007/s00374-007-0169-y

Schomberg, H.H., Steiner, J.L., Unger, P.W., 1994. Decomposition and Nitrogen Dynamics of Crop Residues: Residue Quality and Water Effects. Soil Science Society of America Journal 58, 372–381. doi:10.2136/sssaj1994.03615995005800020019x

Sinsabaugh, R.L., Manzoni, S., Moorhead, D.L., Richter, A., 2013. Carbon use efficiency of microbial communities: stoichiometry, methodology and modelling. Ecology Letters 16, 930–939. doi:10.1111/ele.12113

Sukitprapanon, T.-S., Jantamenchai, M., Tulaphitak, D., Vityakon, P., 2020. Nutrient composition of diverse organic residues and their long-term effects on available nutrients in a tropical sandy soil. Heliyon 6, e05601. doi:10.1016/j.heliyon.2020.e05601

Trinsoutrot, I., Recous, S., Bentz, B., Linères, M., Chèneby, D., Nicolardot, B., 2000. Biochemical

879 Quality of Crop Residues and Carbon and Nitrogen Mineralization Kinetics under Nonlimiting
880 Nitrogen Conditions. Soil Science Society of America Journal 64, 918–926.
881 doi:10.2136/sssaj2000.643918x

882 Van Soest, P.J., 1963. Use of Detergents in the Analysis of Fibrous Feeds. I. Preparation of Fiber
883 Residues of Low Nitrogen Content. J. Assoc. Off. Anal. Chem. 46, 825–835.
884
885 Wang, C., Wang, X., Pei, G., Xia, Z., Peng, B., Sun, L., Wang, J., Gao, D., Chen, S., Liu, D., Dai, W.,
886 Jiang, P., Fang, Y., Liang, C., Nanping, W., Bai, E., 2020. Stabilization of microbial residues in
887 soil organic matter after two years of decomposition. Soil Biology and Biochemistry 141,
888 107687. doi:10.1016/j.soilbio.2019.107687

889 Wang, W.J., Baldock, J.A., Dalal, R.C., Moody, P.W., 2004. Decomposition dynamics of plant
890 materials in relation to nitrogen availability and biochemistry determined by NMR and wet-
891 chemical analysis. Soil Biology and Biochemistry 36, 2045–2058.
892 doi:10.1016/j.soilbio.2004.05.023

893 Yansheng, C., Fengliang, Z., Zhongyi, Z., Tongbin, Z., Huayun, X., 2020. Biotic and abiotic nitrogen
894 immobilization in soil incorporated with crop residue. Soil and Tillage Research 202, 104664.
895 doi:10.1016/j.still.2020.104664

896 Zechmeister-Boltenstern, S., Keiblinger, K.M., Mooshammer, M., Peñuelas, J., Richter, A., Sardans,
897 J., Wanek, W., 2015. The application of ecological stoichiometry to plant–microbial–soil organic
898 matter transformations. Ecological Monographs 85, 133–155. doi:10.1890/14-0777.1

899

900 **Figure captions**

901 Fig. 1. Cumulative apparent mineralization of C (a, b) and N (c, d) during the decomposition of 10
902 crop residues in the soil. Crop residues were either incorporated (I) or left on the soil surface
903 (S). The initial mineral N content was 9 mg N kg^{-1} dry soil (9 N) or 77 mg N kg^{-1} dry soil (77
904 N). These two factors resulted in 4 different treatments.

905 Fig. 2. Cumulative apparent C mineralization (a, b, c) and net N mineralization (d, e, f) and the
906 relationship between N and C mineralization (g, h, i) for three crop residues (wheat, vetch,
907 oilseed rape) in four treatments (I-77N, I-9N, S-77N, S-9N) during decomposition in soil at
908 25°C for 120 days. Bars represent the standard deviation values (*n*=3).

909 Fig. 3. Observed and simulated apparent C mineralization during the decomposition of wheat (a, b, c,
910 d), vetch (e, f, g, h) and oilseed rape (i, j, k, l) residues incorporated or at the soil surface and
911 with high or low initial soil mineral N content (77 or 9 mg N kg^{-1} dry soil) (symbols). Lines
912 represent the values simulated with STICS default parameters (dashed lines) and optimized
913 parameters in *scenario 2* (solid lines). Bars represent the standard deviations (*n*=3).

914 Fig. 4. Observed and simulated apparent N mineralization during the decomposition of wheat (a, b, c,
915 d), vetch (e, f, g, h) and oilseed rape (i, j, k, l) residues incorporated or at the soil surface and
916 with high or low initial soil mineral N content (77 or 9 mg N kg^{-1} soil) (symbols). Lines
917 represent the values simulated with STICS default parameters (dashed lines) and optimized
918 parameters in *scenario 2* (solid lines). Bars represent the standard deviations (*n*=3).

919 Fig. 5. Model parameters *k* (day^{-1}), λ (day^{-1}), *h* and *CNbio* obtained by individual fitting procedures
920 (scenario 2: *k, λ, h, CNbio* and *CNhum*) vs. total N availability (kg N t^{-1} added C) for the dataset
921 of 40 incubations (10 residues, surface vs. incorporated and high vs. low N availability). Lines
922 represent the nonlinear regression fit. The symbol ** indicates that the Pearson coefficient r is
923 significant at the 1% level.

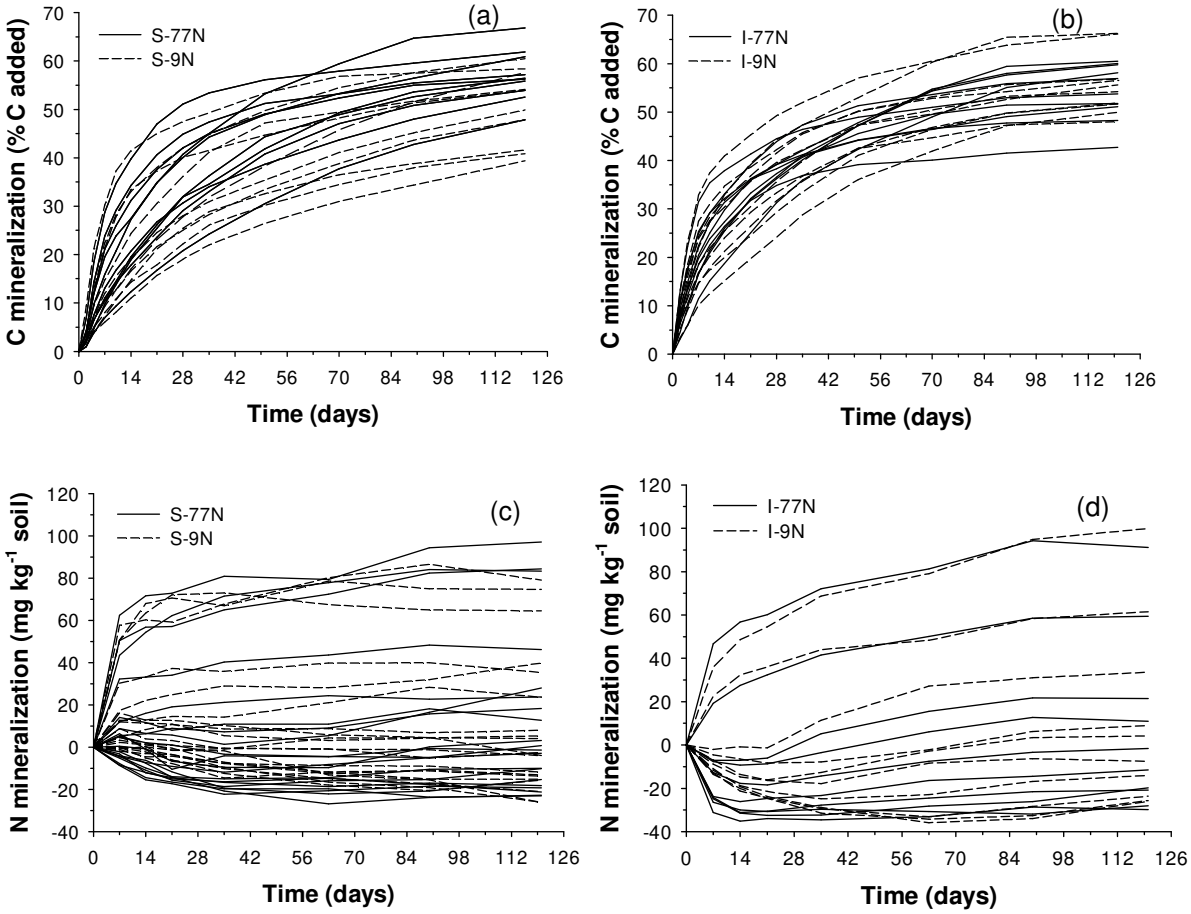

Fig. 1. Cumulative apparent mineralization of C (a, b) and N (c, d) during decomposition of 10 crop residues in the soil. Crop residues were either incorporated (I) or left at the soil surface (S). Initial mineral N content is 9 mg N kg^{-1} dry soil (9N) or 77 mg N kg^{-1} dry soil (77N), resulting in 4 different treatments.

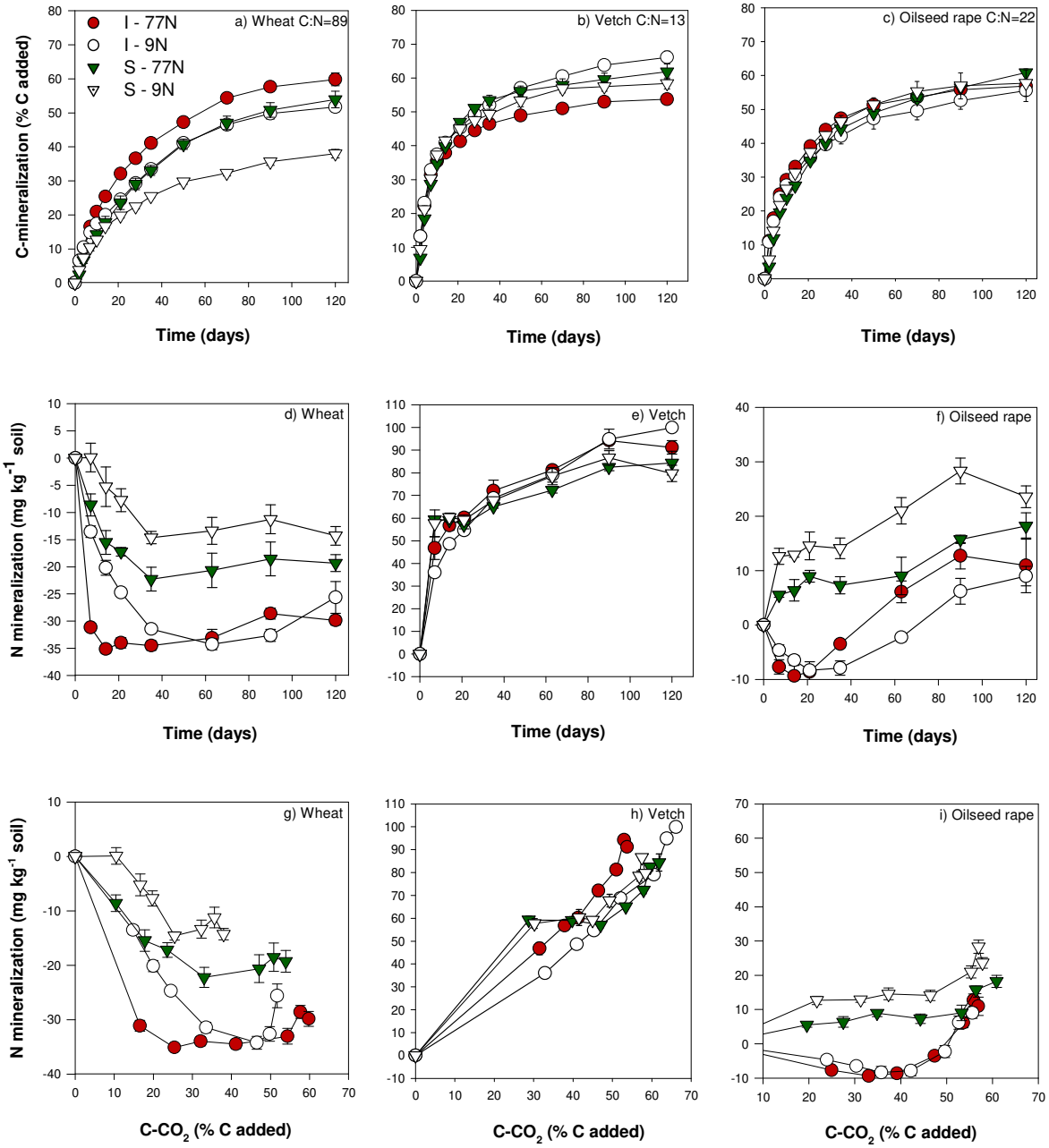

Fig. 2. Cumulative apparent C mineralization (a, b, c), net N mineralization (d, e, f) and the relationship between N and C mineralization (g, h, i) of three crop residues (wheat, vetch, oilseed rape) for four treatments (I-77N, I-9N, S-77N, S-9N) during decomposition in soil at 25°C during 120 days. Bars are standard deviation values (*n*=3).

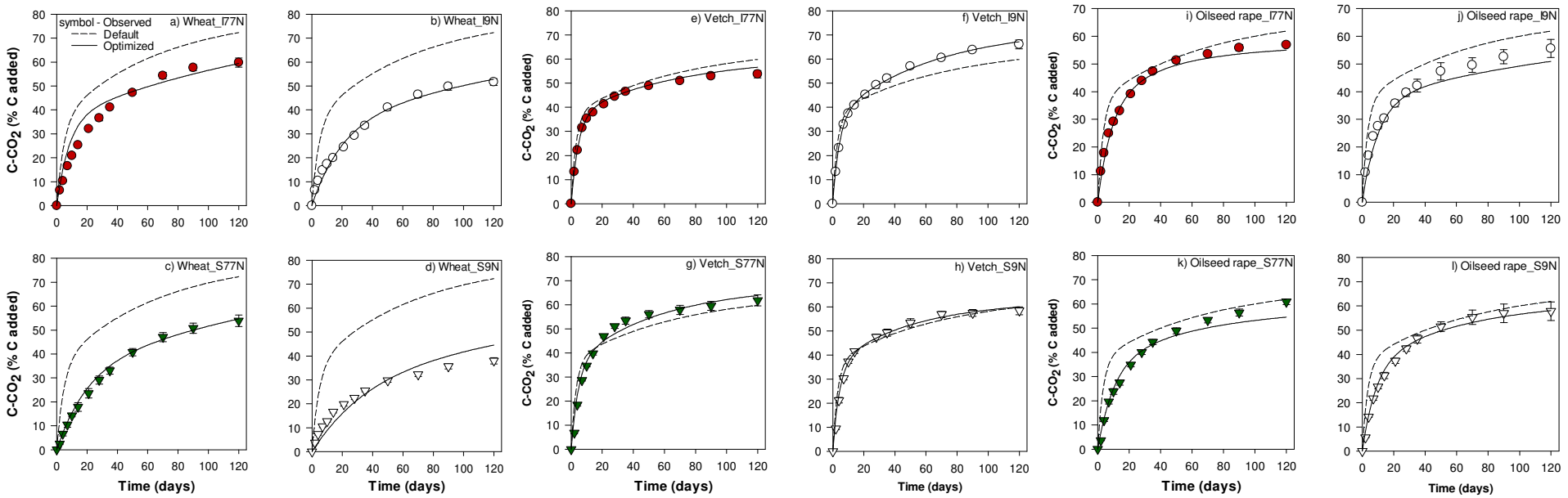

Fig. 3. Observed and simulated apparent mineralization of C during the decomposition of wheat (a, b, c, d), vetch (e, f, g, h) and oilseed rape (i, j, k, l) residues, incorporated or at soil surface and with high or low initial soil mineral N content (77 or 9 mg N kg^{-1} dry soil) (symbols). Lines represent the values simulated with STICS default parameters (dashed lines) and optimized parameters in *scenario 2* (solid lines). Bars are standard deviations (*n*=3).

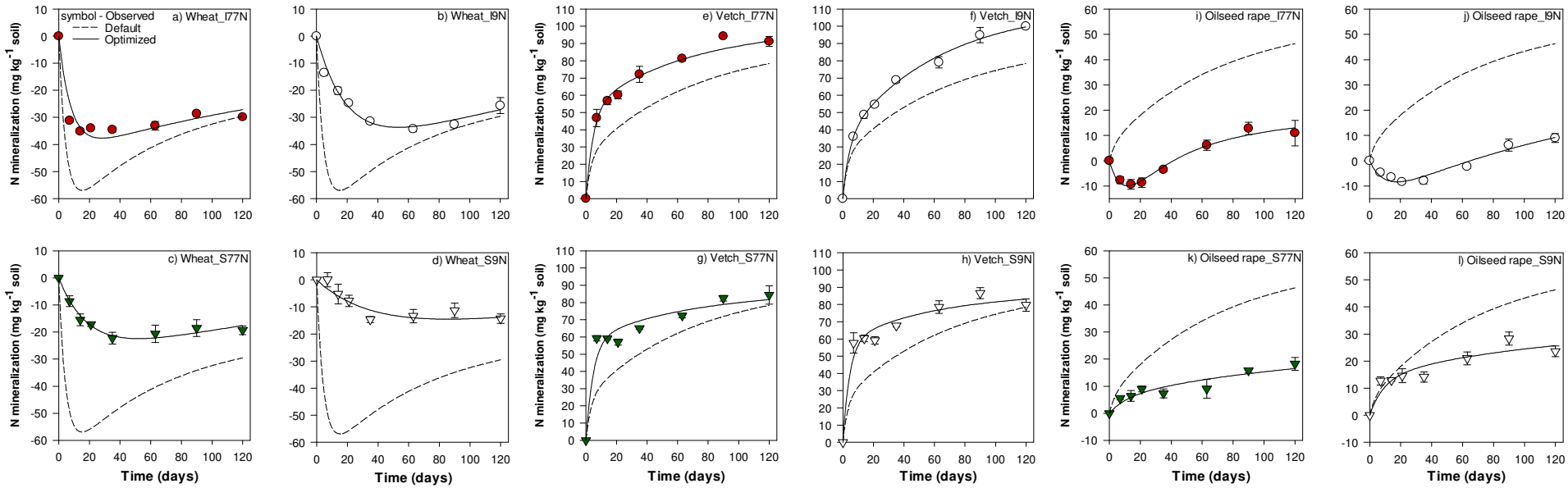

Fig. 4. Observed and simulated apparent mineralization of N during the decomposition of wheat (a, b, c, d), vetch (e, f, g, h) and oilseed rape (i, j, k, l) residues, incorporated or at soil surface and with high or low initial soil mineral N content (77 or 9 mg N kg^{-1} soil) (symbols). Lines represent the values simulated with STICS default parameters (dashed lines) and optimized parameters in *scenario 2* (solid lines). Bars are standard deviations (n=3).

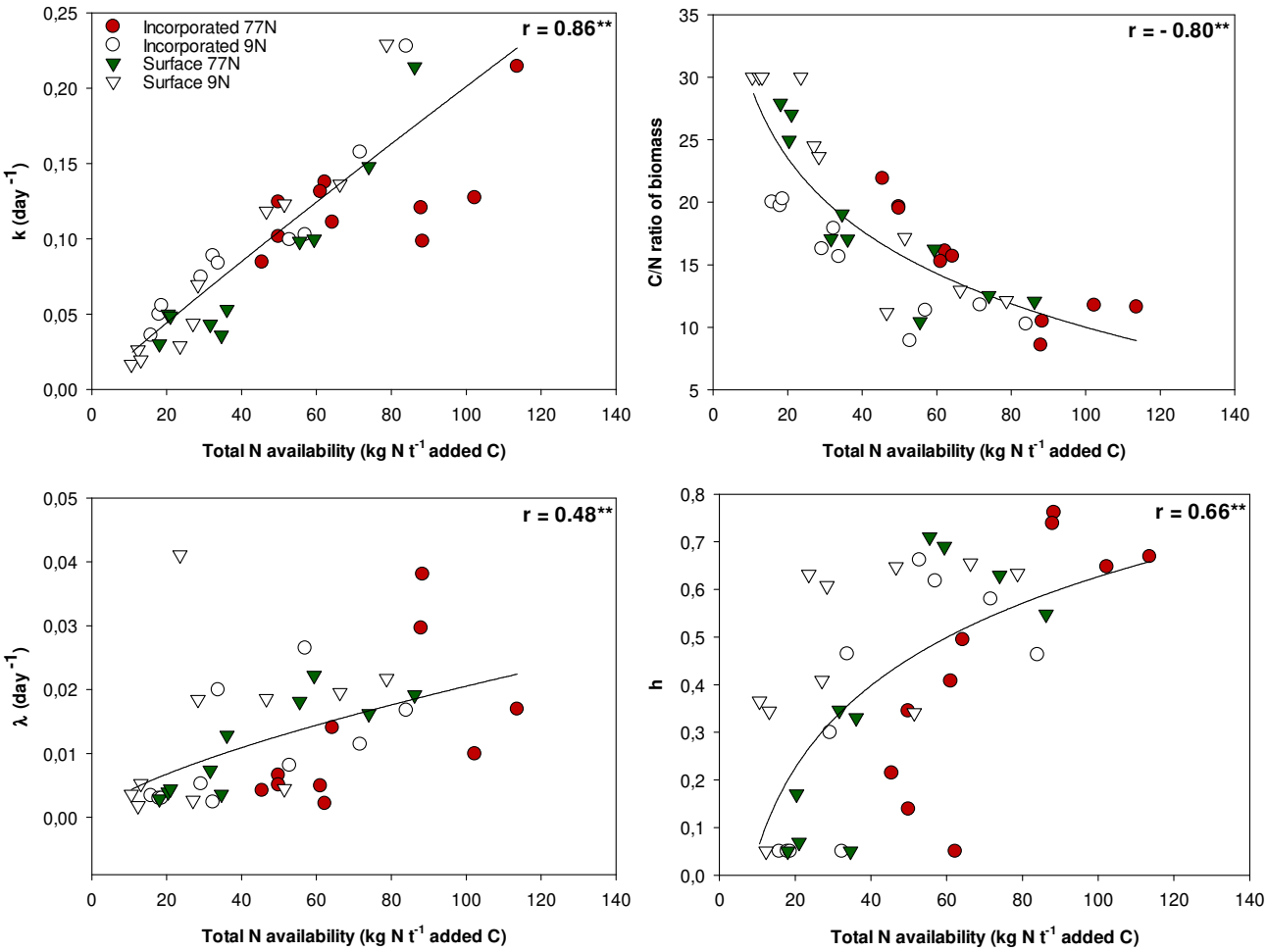

Fig. 5. Model parameters *k* (day^{-1}), λ (day^{-1}), *h* and *CNbio* obtained by individual fitting procedure (scenario 2: *k, λ, CNbio, CNhum, h*) vs. N availability (kg N t^{-1} added C) for the dataset of 40 incubations (10 residues, surface vs. incorporated and high vs. low N availability). Symbol ** mean that Pearson coefficient r is significant at the 1% level.

Table 1. Crop residues used, proportion of their leaves and stems in the mixture (% total of DM) and their initial chemical composition (g kg^{-1} DM).

Latin name	Common name	Agricultural use	% leaf[a]	% stem[a]	SOL[b]	HEM[b]	CEL[b]	LIG[b]	Total C[b]	Total N[b]	C:N ratio
Brassica napus oleifera	Oilseed rape	Main crop	28 ± 3.6	72 ± 2.8	394 ± 8.4	152 ± 4.1	359 ± 14.1	95 ± 2.5	421 ± 6.5	19.1 ± 2.3	22
Glycine max	Soybean	Main crop	38 ± 3.2	62 ± 2.1	349 ± 8.5	122 ± 3.4	386 ± 2.2	143 ± 1.4	450 ± 6.2	11.7 ± 3.4	38
Helianthus annuus	Sunflower	Main crop	39 ± 4.2	61 ± 5.1	322 ± 2.5	79 ± 3.7	485 ± 7.8	114 ± 0.5	428 ± 7.9	9.6 ± 2.8	45
Hordeum vulgare	Barley	Main crop	50 ± 3.3	50 ± 2.0	271 ± 3.5	260 ± 6.6	407 ± 8.7	62 ± 4.5	441 ± 0.7	5.3 ± 0.8	83
Triticum aestivum	Wheat	Main crop	42 ± 4.1	58 ± 3.3	326 ± 11.2	257 ± 10.2	356 ± 3.5	61 ± 6.3	437 ± 0.8	4.9 ± 4.5	89
Zea mays	Maize	Main crop	26 ± 3.6	74 ± 3.9	141 ± 6.3	323 ± 9.5	469 ± 10.1	67 ± 0.7	452 ± 2.4	4.3 ± 5.5	105
Avena strigosa	Black oat	Cover crop	48 ± 2.0	52 ± 2.7	290 ± 5.4	246 ± 8.2	417 ± 12.1	47 ± 0.3	447 ± 4.3	12.2± 4.3	37
Crotalaria spectabilis	Showy rattlebox	Cover crop	30 ± 3.1	70 ± 3.1	417 ± 2.6	90 ± 2.4	408 ± 8.9	85 ± 1.9	445 ± 5.1	22.4 ± 4.2	20
Stizolobium niveum	Gray mucuna	Cover crop	42 ± 3.6	58 ± 2.9	464 ± 7.9	119 ± 13.2	318 ± 6.6	99 ± 3.6	451 ± 3.3	29.4 ± 1.1	15
Vicia sativa	Vetch	Cover Crop	62 ± 1.8	38 ± 3.5	571 ± 3.9	88 ± 3.7	272 ± 2.3	69 ± 1.1	453 ± 1.6	35.2 ± 6.1	13

[a] Proportion of leaves and stems in the total dry matter of shoots determined at flowering for cover crops and harvest for main crops .
[b] SOL: Soluble fraction (Van Soest); HEM: Hemicellulose; CEL: Cellulose; LIG: Lignin; C: Total organic carbon; N: Total nitrogen; Csw: Water-soluble carbon; Nsw: Water-soluble nitrogen; C:N ratio is the ratio between Total C and Total N. Means (n = 3) $\pm$ standard deviation (S.D.).

Table 2. Statistical analysis (RMSE) of default parameter values and of parameters after optimization using four scenarios with the STICS decomposition module.

Optimization Scenarios	Parameters optimized	RMSE (C)[a] % added C	RMSE (N)[a] mg N kg^{-1}soil
Default	-	13.05	18.81
1	*k, λ, CNbio* and *CNhum*	3.00	2.28
2	*k, λ, CNbio, CNhum and h*	2.40	2.00
3	*k, λ, CNbio, CNhum, h and Y*	2.03	1.83

[a]mean of the 40 incubations dataset.